Electronic Supporting Information (ESI) for the paper:

Crossed-Beam and Theoretical Studies of Multichannel Nonadiabatic Reactions: Branching Fractions and Role of Intersystem Crossing for O(^{3}P) + 1,3-Butadiene

C. Cavallotti,[1*] A. Della Libera,[1] Chong-Wen Zhou,[2,3] P. Recio,[4] A. Caracciolo,[4] N. Balucani[4] and P. Casavecchia[4*]

[1]*Dipartimento di Chimica, Materiali e Ingegneria Chimica "Giulio Natta", Politecnico di Milano, 20131 Milano, Italy. E-mail:* carlo.cavallotti@polimi.it

[2]*School of Energy and Power Engineering, Beihang University, Beijing 100191, PR China*

[3]*Combustion Chemistry Centre, School of Chemistry, Ryan Institute, National University of Ireland, Galway, Galway H91TK33, Ireland*

[4]*Dipartimento di Chimica, Biologia e Biotecnologie, Università degli Studi di Perugia, 06123 Perugia, Italy. E-mail:* piergiorgio.casavecchia@unipg.it

This file contains:

S1. Crossed-beam experimental results for O(^{3}P) + 1,3-Butadiene

The bimolecular reaction of O(^{3}P) with 1,3-Butadiene exhibits a large variety of energetically open (exothermic) reaction channels. Experimentally, using the crossed molecular beam (CMB) technique with mass-spectrometric (MS) detection and time-of-flight (TOF) analysis, and exploiting soft electron ionization for product detection as described in the main text, we have probed the following eight channels at E_c=32.6 kJ/mol:

$O(^3P) + C_4H_6$	$\rightarrow$	$CH_2CHCHCHO + H$	$\Delta H_0^0 = -106.7$ kJ/mol	(1a)
	$\rightarrow$	$CH_2CHCOCH_2 + H$	$\Delta H_0^0 = -70.3$ kJ/mol	(1b)
	$\rightarrow$	$CH_2CHCHCO + H_2$	$\Delta H_0^0 = -338.5$ kJ/mol	(2)
	$\rightarrow$	$C_3H_6 + CO$	$\Delta H_0^0 = -455.2$ kJ/mol	(3)
	$\rightarrow$	$CH_2CO + C_2H_4$	$\Delta H_0^0 = -359.4$ kJ/mol	(4)
	$\rightarrow$	C_3H_5 (allyl) + HCO	$\Delta H_0^0 = -153.6$ kJ/mol	(5)
	$\rightarrow$	$CH_2CHO + C_2H_3$	$\Delta H_0^0 = -49.4$ kJ/mol	(6)
	$\rightarrow$	$CH_3CO + C_2H_3$	$\Delta H_0^0 = -77.4$ kJ/mol	(7)
	$\rightarrow$	$H_2CO + C_3H_4$(allene)	$\Delta H_0^0 = -283.3$ kJ/mol	(8a)
	$\rightarrow$	$H_2CO + CH_2CHCH$ (vinylmethylene)	$\Delta H_0^0 = -61.5$ kJ/mol	(8b)

Here, the reaction enthalpies are those derived from the present electronic structure calculations (accuracy ±4 kJ/mol) (see Fig. 1 in main text).

As discussed in the main text, there also two different CH_3 elimination channels, leading to CH_3+CH_2CHCO and CH_3+CHCHCHO, which are also exothermic ($\Delta H_0^0 = -122.6$ *and* -33.5 kJ/mol, respectively) (see Fig. 1 in main text). We attempted to probe these channels by detecting the methyl radical (*m/z*=15). However, no reactive signal was observed within our sensitivity, and this puts its BF at $\leq$ 1% - 2%. Neither the direct H abstraction forming OH has been observed at *m/z*=17. The OH channel, even though is slightly

exothermic ($\Delta H_0^0 = -9.2\ kJ/mol$), is characterized by a high entrance barrier of 31.8 kJ/mol, which makes it negligible under our experimental conditions of E_c=32.6 kJ/mol. This conclusion is corroborated by the theoretical kinetic calculations that have determined the channel specific abstraction rate constant as a function of temperature to be negligible at room temperature and still much lower than the addition rate constants even at 1000 K (see Fig. 4 in Main Text).

We wish to note that the small percentage (≤10%) of O(^{1}D) present in the atomic oxygen beam[1] is expected to contribute negligibly to the results because the reactivity of O(^{3}P) (dominant in the beam) becomes comparable to that of O(^{1}D) at this high collision energy, and presumably, as for the case of the reaction O+C_2H_2,[2] the O(^{1}D) reaction mainly would produce OH + C_5H_5. Therefore, the contribution of O(^{1}D) is assumed to be negligible in the present study.

The velocity vector (so called "Newton") diagram of the CMB experiment is depicted in Fig. S1a. It describes the kinematics of the reactive system. There, the circles superimposed on the diagram, and concentric to the center-of-mass (CM) position, delimit the maximum CM velocity that the indicated primary products can attain by assuming that all the available energy (given by $E_c - \Delta H_0^0$) is channeled into product translational energy. From this diagram we can see that the heavy co-product of channel (1) is extremely enhanced in the LAB frame because of the very favorable CM→LAB transformation Jacobian[3,4] for the heavy co-product of the H channel with respect to lighter products left by a heavy co-product (see below).

We have observed reactive signal at the following mass-to-charge (*m/z*) ratios: *m/z*=69 ($C_4H_5O^+$), 68 ($C_4H_4O^+$), 43 ($C_2H_3O^+$), 42 ($C_3H_6^+$, CH_2CO^+), 41 ($C_3H_5^+$), 30 (CH_2O^+), and 29 (HCO^+), with relative intensities at the CM angle (using 17 eV electron energy) of 0.04, 0.21, 0.02, 0.14, 1.00, 0.12 and 0.13, respectively. The product LAB angular distributions, N(Θ), were acquired only at *m/z*=69, 68, 43, 42, 41, and 29, while not at *m/z*=30 for poor S/N reasons; they are reported in Fig. 1b. Due to the low signal-to-noise (S/N), at *m/z*=69 and 43 only angular distributions were measured. Instead for *m/z*=30, only (two) TOF distribution were recorded because of the low signal-to-noise (S/N) ratio in the angular distribution. Most measurements were carried out exploiting soft electron ionization at 17 eV electron energy, which was sufficient to suppress most of the interferences from dissociative ionization processes of

reactants and background gases. However, for some masses data were collected at both 70 eV and 17 eV for normalization purposes.

The Figures S2a and S2b show the TOF distributions at *m/z*=68 and *m/z*=41, respectively, for six different LAB angles, while Fig. S2c shows the TOF data at *m/z*=42 at only two LAB angles. The TOF spectra at *m/z*=29 at four different LAB angles are instead shown in Fig. S3(*rhs*),

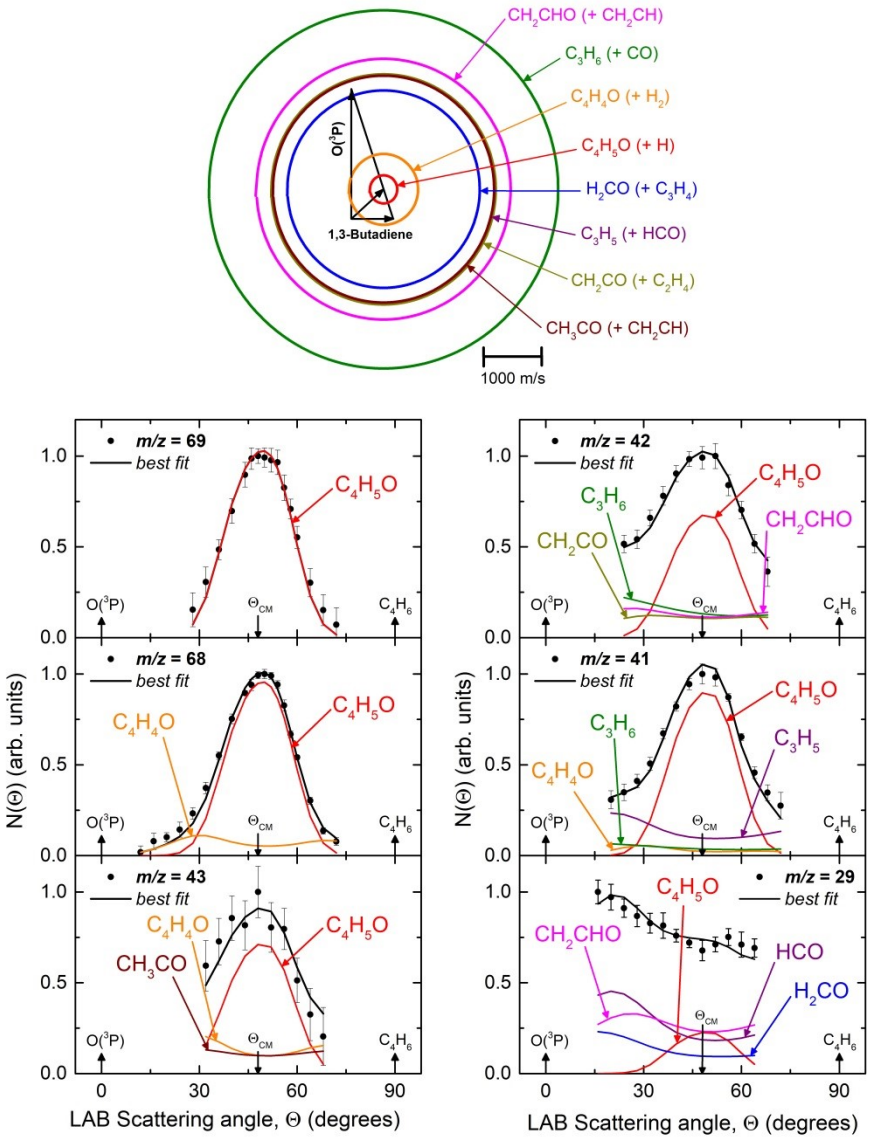

Fig S1 (a) Velocity vector diagram for the $O(^3P)$+1,3-butadiene reaction (E_c=32.6 kJ/mol) where the color coded circles concentric to the CM delimit the maximum velocity that the indicated primary products can attain in the CM frame on the basis of energy and momentum conservation, assuming that all the total available energy is channeled into recoil energy of the products (i.e., assuming that the products are formed in their lowest ro-vibrational state). Eight different reactive channels were identified, C_4H_5O+H (red); C_4H_4O+H_2 (orange); C_3H_6+CO (green); C_3H_5+HCO (purple); CH_2CO+C_2H_4 (green-olive); CH_2CHO+C_2H_3 (pink), CH_3CO+CH_2CH (garnet), and

$H_2CO+C_3H_4$ (blue). (b) LAB angular distributions N(Θ) measured at *m/z*=69, 68, 43 (*lhs*) and 42, 41, 29 (*rhs*). The black solid line superimposed on the experimental data (black dots) corresponds to the calculated global best-fit using the CM functions depicted in Fig. S4. The distinct contributions to the calculated global N(Θ) are colored coded ad in Fig. 1a and indicated with the formula of the corresponding product. Experimental error bars represent ±1σ.

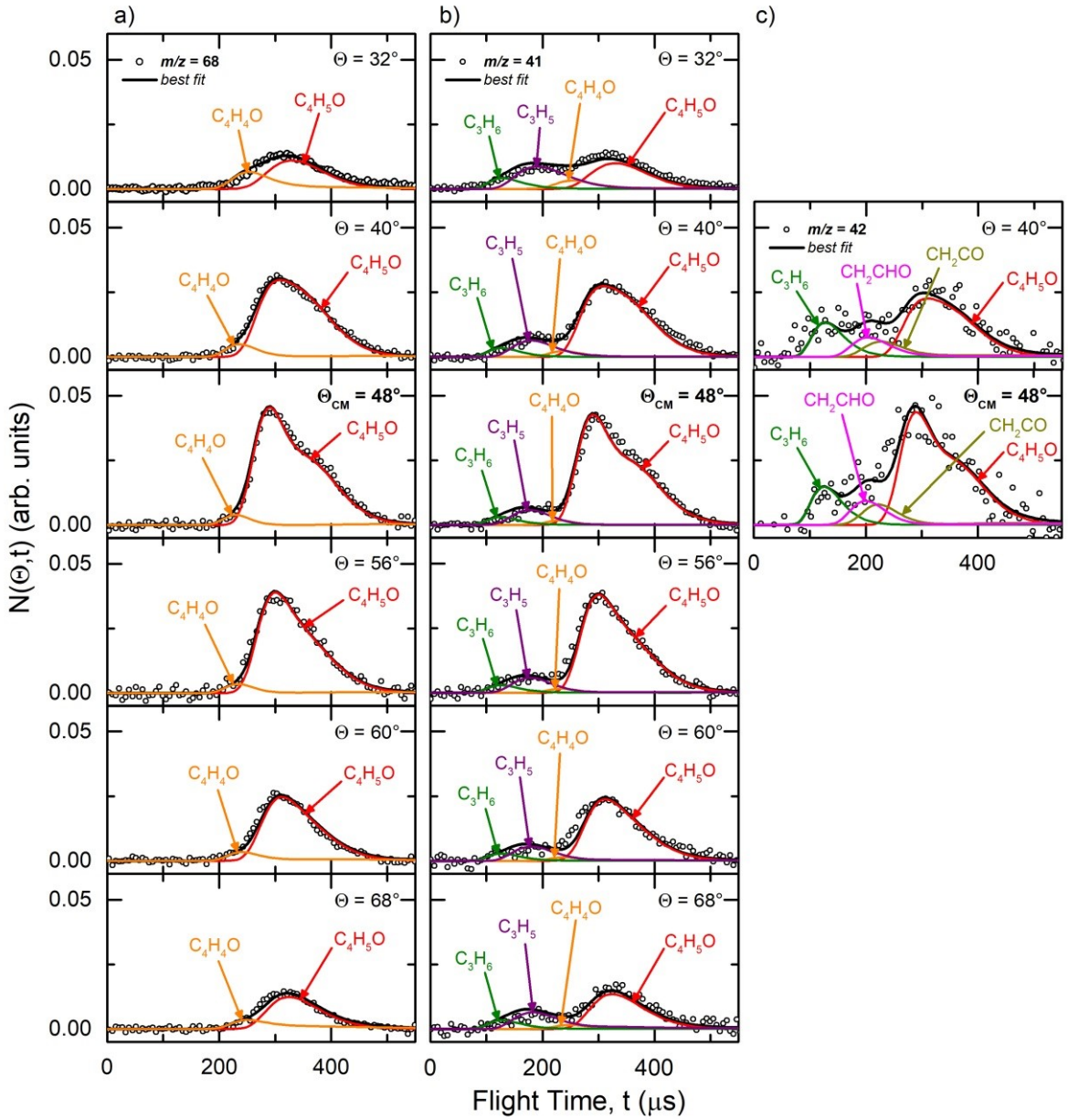

Fig S2 Product TOF distributions for (a) *m/z*=68 (at 70 eV), (b) *m/z*=41 (at 17 eV), and (c) *m/z*=42 (at 17 eV) at the indicated LAB angles Θ. The distinct contributions of the different products contributing at each of the three

masses are indicated. Color coding as in Fig. S1. Note that the integrated signal at Θ_{CM}=48° (at 17 eV) for *m/z*=41 is seven times larger than for *m/z*=42, and five times larger than for *m/z*=68, as reflected in the S/N of the spectra.

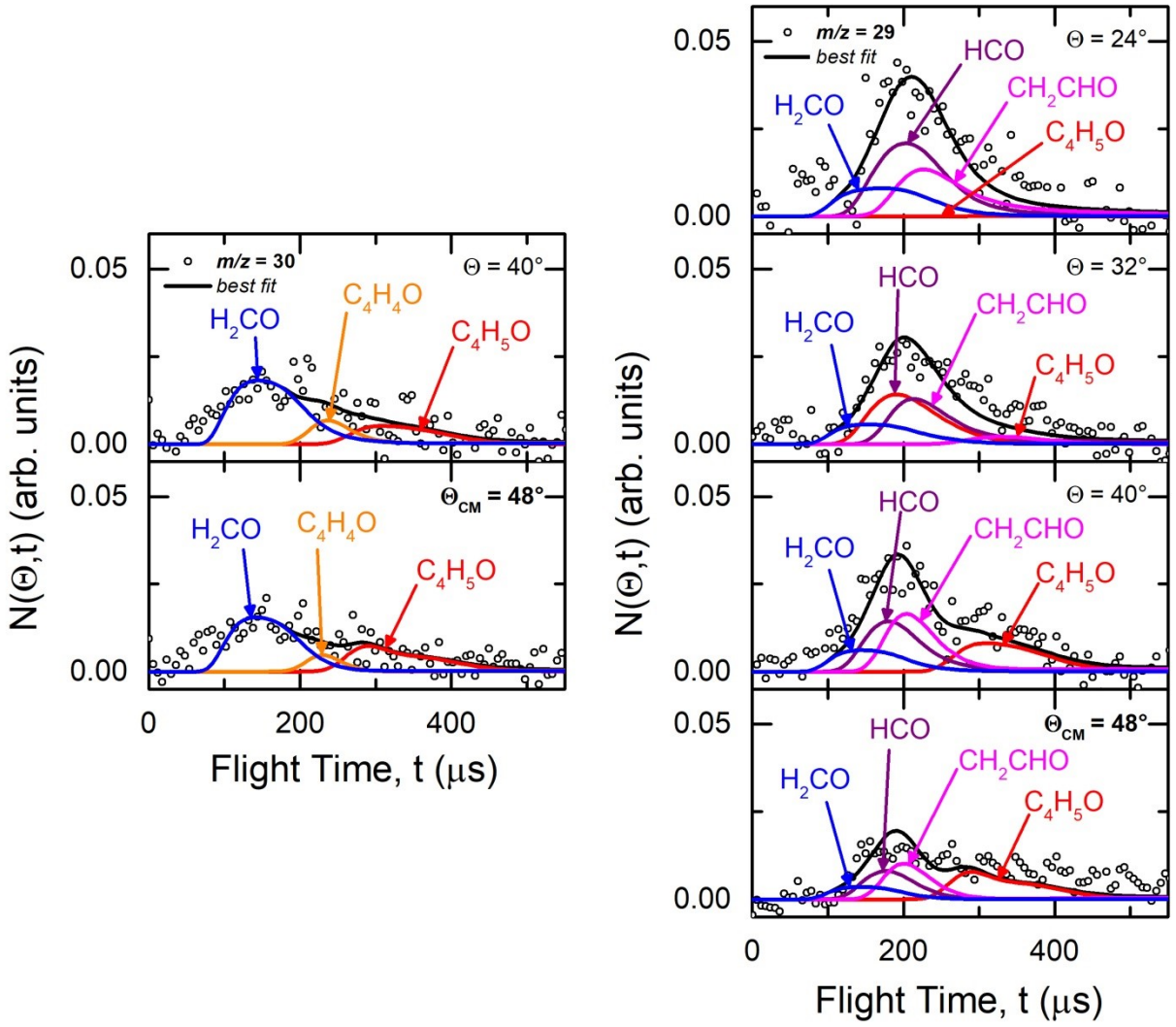

Fig S3 Product TOF distributions measured for *m/z*=30 at LAB angles of 40° and 48° with hard ionization (70 eV) (*lhs*) and *m/z*=29 at LAB angles 24°, 32°, 40°, and 48° with soft ionization (17 eV) (*rhs*). Distinct product contributions are indicated. Color coding as in Figs. S1 and S2.

and those at *m/z*=30 at two LAB angles in Fig. S3(*lhs*). Typical measuring times ranged from two to four hours for each TOF spectrum. The black continuous curves in Figs S1-S3 represent the global best-fit for the indicated *m/z* data, while the labeled color coded curves are the partial

contributions from the various indicated products, when using the best-fit CM product angular, $T(\theta)$, and translational energy, $P(E'_T)$, distributions reported in Fig. S4.

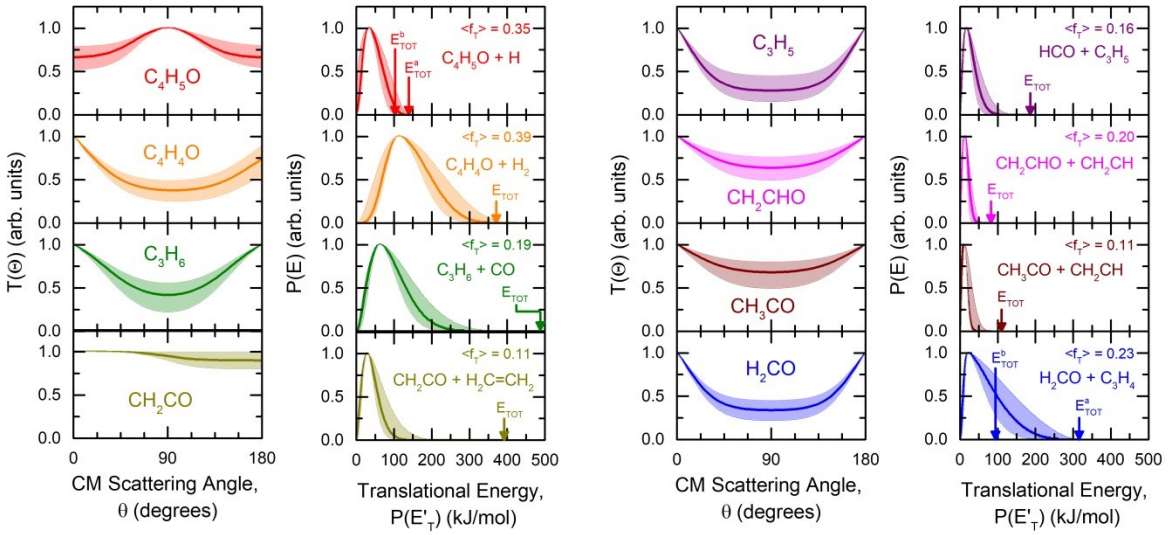

Fig. S4 CM best-fit functions for the $O(^3P)$ + 1,3-butadiene reaction at E_c=32.6 kJ/mol. 1st and 3rd panel (from left): best-fit CM angular distributions of C_4H_5O, C_4H_4O, propene (C_3H_6), ketene (CH_2CO), allyl (C_3H_5), vinoxy (CH_2CHO), acetyl (CH_3CO), and formaldehyde (H_2CO). 2nd and 4th panel: best-fit CM translational energy distributions for each corresponding channel. Color coding as in Figs. S1-S3. The total energy (E_{TOT}) and the average translational energy fraction ($\langle f_T \rangle$) (referred to the most exothermic isomeric channel) determined for each reaction channel are indicated. In the top and bottom sub-panels of 2nd and 4th panel (from left) the two arrows refer to the two different isomeric channels (1a) and (1b), and (8a) and (8b), respectively. The shaded areas represent the error bars determined for the best-fit CM functions.

The information content of the $N(\Theta)$ and $N(\Theta,t)$ data about the complex reaction dynamics of $O(^3P)$ + 1,3-butadiene has been discussed in some detail in the Main Text. The derived best-fit CM functions (see Fig. S4) contain all the information about the dynamics of formation of the 8 competing product channels.

The interpretation of the CMB results has been synergistically assisted by high-level electronic structure calculations of the underlying triplet and singlet PESs for the C_4H_6O system (see Fig. 1 in Main Text). Besides identifying 8 competing product channels, we have been able to also estimate experimentally the branching fractions of the different product channels (see Table 1 in Main Text). Furthemore, for some channels we have been able to observe also peculiar dynamical features, such as in the case of the H-displacement channels (1).

Stereodynamics of channels (1): $O(^3P) + C_4H_6 \rightarrow C_4H_5O + H$.

Experimentally it was not possible to distinguish the relative contributions of channel (1a) and channel (1b), being the dynamics similar and the resolution of this experiment not sufficient. However, theory has predicted that at the experimental E_c channel (1b) gives a contribution of about 15% to the total H yield (the contribution increases with increasing E_c (or temperature)) (see Table 1 in Main Text). The fact that the T(θ) of the H-displacement channel is different from that of all the other channels and, in particular, has a maximum at θ=90° rather than a minimum (see Fig. S4), indicates that the H atom departs orthogonally to the molecular plane at the transition state.[5-7] This is nicely corroborated by the theoretical finding that the calculated geometry of the exit transition state, following both O atom attack to the terminal carbon (most favored) and O atom attack to the central carbon, indicates that the angle that the H-atom forms with respect to the molecular plane, when leaving ^{3}TS2 (following C1 attack) is about 105°, while it is about 88° when it leaves ^{3}TS10 following C2 attack (see Fig. S5 and also Fig. 1a of the triplet PES in the Main Text). Being the T(θ) perfectly symmetric, *i.e.*, having the same intensity at θ=0° (forward direction with respect to the incoming O atom in the CM) and θ=180° (backward direction), indicates that the reaction forming H atoms on the triplet PES proceeds via a long-lived complex mechanism,[5-7] that is via a complex (^{3}W1 and ^{3}W2 in our case, see Fig. 1a in Main Text) whose average lifetine is longer (≥ 5-6) than the average rotational period of the dissociating complex. Notably, a similar sideways scattering dynamics has been observed also for the CH_3 elimination channel in the reaction $O(^3P)$ + toluene where, at a comparable E_c, the CH_3 group leaves the aromatic ring at nearly 90° at the exit transition state, forming CH_3 + C_6H_5O (phenoxy).[8]

It is also worth commenting that the C_4H_5O + H channel, despite the very high signal in the laboratory of the C_4H_5O co-product (detected at its parent mass and its daughter ion masses) contributes for less than 10% to the total product yield of the $O(^3P)$+1,3-butadiene reaction at E_c=32.6 kJ/mol (see Table 1 in Main Text). In particular, the main daughter ion of C_4H_5O occurs at *m/z*=41 ($C_3H_5^+$) which arises by the following dissociative ionization process (even at 17 eV): $C_4H_5O + e^- \rightarrow C_3H_5^+ + CO$. The high intensity at *m/z*=41 due to the H displacement channel is

well visible both in the N(Θ) and in the TOF spectra. The fast peak at *m/z*=41 at around 180 μs, much faster than the $C_3H_5^+$ component from channel (1) via the above dissociative ionization process, appears much less intense in the LAB frame with respect to the latter, despite the C_3H_5 (allyl) (*m/z*=41) product from channel (5) has a reactive integral cross section about a factor of 6 larger, the reason being that by momentum conservation C_3H_5 from channel (5) is scattered over a much larger Newton circle than C_4H_5O (detected at *m/z*=41) from channel (1). A similar situation occurs also for channel (6) (C_3H_6 + CO), but in this case the fragmentation of C_4H_5O to *m/z*=42 is much lower than at *m/z*=41 (see Fig. S2c).

It should also be noted that, because the detector acceptance angle is the same for all channels, about 1°, in this type of experiments, at a given LAB angle a much smaller slice of a large Newton circle is being detected with respect to the case of a small Newton circle. We recall that the actual product distribution of a product in the LAB as well in the CM, occurs on a 3-D sphere because of the cylindrical symmetry of the scattering process, when using non polarized atomic and molecular beams, as in our case.[9] In fact, because of the cylindrical symmetry of the scattering process, detection can be made, using a high angular resolution (tipically 1°), in the plane of the sphere at the equator, that is the plane of a circle (see Fig. S1a), by rotating the detector in the plane defined by the two intersecting molecular beams, around the axis orthogonal to the collision plane and passing through the collision center.[3,4,9]

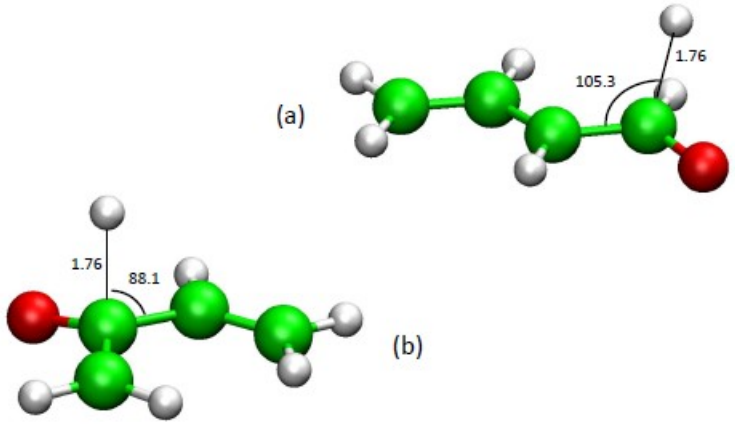

Fig. S5 Transition state structures from the present electronic structure calculations (see sect. 2.2 in Main Text). (a): ^{3}TS2, (b): ^{3}TS10 (see triplet PES in Fig. 1a of Main Text). The C-H distance at the transition state is in Å.

S2. Thermal Rate constants (0.1, 1, 10 atm and 300-2200 K)

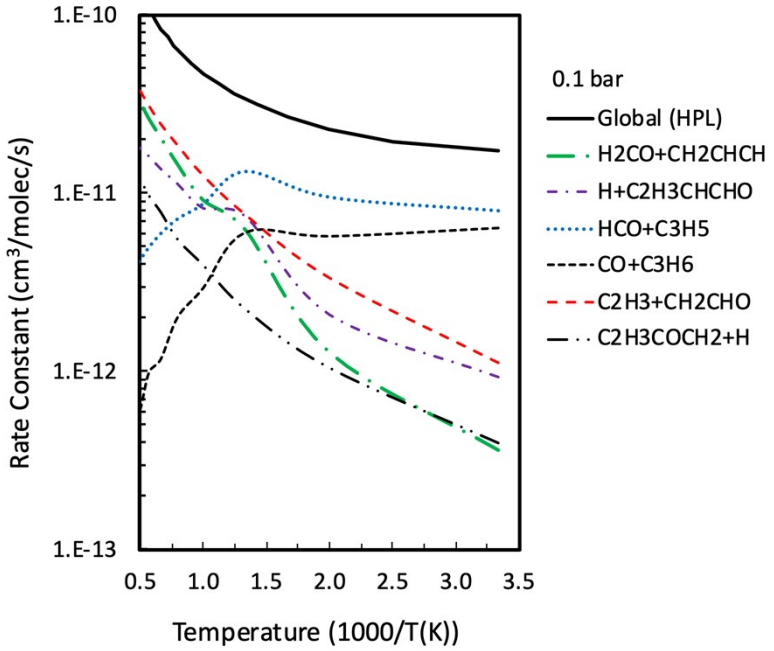

Fig. S6. Channel specific rate constants computed as a function of temperature at 0.1 bar.

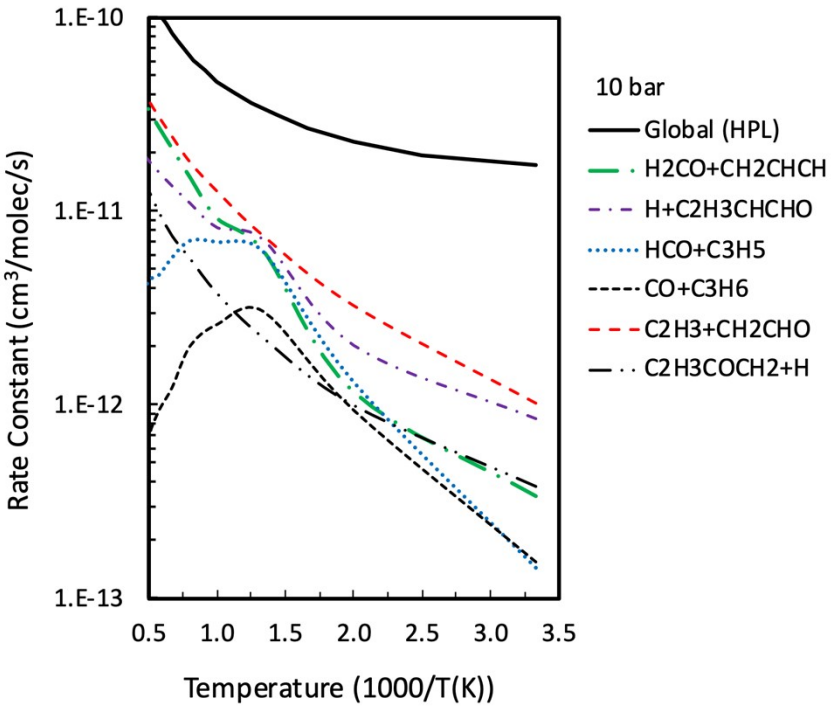

Fig S7. Channel specific rate constants computed as a function of temperature at 10 bar.

Table S1. Rate constants computed through ME simulations in an Ar bath gas at 0.1 bar.

T(K)	H_2CO+CH_2CHCH	$H+C_2H_3CHCHO$	$HCO+C_3H_5$	$CO+C_3H_6$	W2	W3	$C_2H_3+CH_2CHO$	$C_2H_3COCH_2+H$	Total
300	3.65E-13	9.26E-13	7.99E-12	6.39E-12	6.84E-14	1.78E-14	1.11E-12	3.96E-13	1.73E-11
500	1.29E-12	2.07E-12	9.50E-12	5.74E-12	4.55E-15	3.03E-15	3.33E-12	1.04E-12	2.30E-11
750	6.31E-12	7.40E-12	1.33E-11	6.03E-12	0.00E+00	0.00E+00	7.56E-12	2.24E-12	4.28E-11
1000	9.24E-12	8.20E-12	8.70E-12	2.94E-12	0.00E+00	0.00E+00	1.25E-11	3.96E-12	4.56E-11
1250	1.46E-11	1.12E-11	7.20E-12	2.03E-12	0.00E+00	0.00E+00	1.85E-11	5.50E-12	5.90E-11
1500	2.06E-11	1.36E-11	5.96E-12	1.18E-12	0.00E+00	0.00E+00	2.43E-11	7.82E-12	7.35E-11
1750	2.64E-11	1.61E-11	4.98E-12	9.89E-13	0.00E+00	0.00E+00	3.10E-11	9.72E-12	8.92E-11
2000	3.31E-11	1.79E-11	4.21E-12	6.10E-13	0.00E+00	0.00E+00	3.78E-11	1.21E-11	1.06E-10
2200	3.83E-11	1.94E-11	3.80E-12	7.05E-13	0.00E+00	0.00E+00	4.35E-11	1.35E-11	1.19E-10

Table S2. Rate constants computed through ME simulations in an Ar bath gas at 1 bar.

T(K)	H_2CO+CH_2CHCH	$H+C_2H_3CHCHO$	$HCO+C_3H_5$	$CO+C_3H_6$	W2	W3	$C_2H_3+CH_2CHO$	$C_2H_3COCH_2+H$	Total
300	3.21E-13	9.48E-13	3.50E-12	3.35E-12	5.09E-12	2.57E-12	1.09E-12	3.91E-13	1.73E-11
500	1.24E-12	2.13E-12	7.62E-12	5.20E-12	1.51E-12	9.58E-13	3.22E-12	1.10E-12	2.30E-11
750	6.26E-12	7.40E-12	1.26E-11	6.22E-12	2.65E-13	1.84E-13	7.53E-12	2.30E-12	4.28E-11
1000	9.18E-12	8.23E-12	8.65E-12	3.07E-12	1.76E-14	1.25E-14	1.25E-11	3.94E-12	4.56E-11
1250	1.46E-11	1.14E-11	7.09E-12	1.88E-12	0.00E+00	0.00E+00	1.85E-11	5.56E-12	5.90E-11
1500	2.06E-11	1.38E-11	5.72E-12	1.43E-12	0.00E+00	0.00E+00	2.46E-11	7.42E-12	7.35E-11
1750	2.65E-11	1.61E-11	4.94E-12	9.57E-13	0.00E+00	0.00E+00	3.05E-11	1.02E-11	8.92E-11
2000	3.29E-11	1.79E-11	4.50E-12	6.85E-13	0.00E+00	0.00E+00	3.75E-11	1.22E-11	1.06E-10
2200	3.76E-11	1.98E-11	3.95E-12	6.21E-13	0.00E+00	0.00E+00	4.34E-11	1.37E-11	1.19E-10

Table S3. Rate constants computed through ME simulations in an Ar bath gas at 10 bar.

T(K)	H_2CO+CH_2CHCH	$H+C_2H_3CHCHO$	$HCO+C_3H_5$	$CO+C_3H_6$	W2	W3	$C_2H_3+CH_2CHO$	$C_2H_3COCH_2+H$	Total
300	3.37E-13	8.47E-13	1.45E-13	1.55E-13	1.29E-11	1.49E-12	1.03E-12	3.83E-13	1.73E-11
500	1.16E-12	2.02E-12	1.30E-12	9.42E-13	1.04E-11	2.88E-12	3.27E-12	1.00E-12	2.30E-11
750	6.24E-12	7.16E-12	6.16E-12	3.07E-12	6.97E-12	3.40E-12	7.55E-12	2.24E-12	4.28E-11
1000	9.08E-12	8.22E-12	6.87E-12	2.63E-12	1.34E-12	9.64E-13	1.27E-11	3.76E-12	4.56E-11
1250	1.48E-11	1.10E-11	7.01E-12	2.03E-12	2.58E-13	2.32E-13	1.80E-11	5.70E-12	5.90E-11
1500	2.09E-11	1.35E-11	5.72E-12	1.24E-12	3.43E-14	4.95E-14	2.46E-11	7.49E-12	7.35E-11
1750	2.68E-11	1.59E-11	4.66E-12	9.44E-13	2.27E-14	0.00E+00	3.10E-11	9.88E-12	8.92E-11
2000	3.26E-11	1.82E-11	4.40E-12	7.04E-13	0.00E+00	0.00E+00	3.72E-11	1.26E-11	1.06E-10
2200	3.75E-11	1.99E-11	3.73E-12	4.69E-13	0.00E+00	0.00E+00	4.30E-11	1.45E-11	1.19E-10

S3. Master Equation Inputs

All relevant parameters for the stationary points used in the ME simulations for the triplet PES are reported in the following, while those for the singlet PES are reported in a companion tar archive. For the relative energies please refer to those reported in the paper.

```
TRIPLET PES

Well W1
 Species
 RRHO
 Geometry[angstrom]            11
  C       0.000000000000     0.000000000000     0.000000000000
  C       0.000000000000     0.000000000000     1.492704212303
  C       1.155458783516     0.000000000000     2.244924763724
  O      -0.779101618179    -0.969994211585    -0.560072298715
  H      -0.459161349707     0.936321711311    -0.386368093048
  H       1.019515362745    -0.004138234940    -0.413577878279
  C       1.196408012000     0.004002067474     3.619696777554
  H      -0.967852020051    -0.025388207253     1.979743556100
  H       2.100897352464    -0.000078329259     1.709612549092
  H       2.135405525455     0.005803240680     4.152520349452
  H       0.285770911415     0.002908832472     4.203764194113
       Core    RigidRotor
            SymmetryFactor    1.0000000000000000
       End
 Rotor                         Hindered
 Group  4 5 6
 Axis            1          2
 Symmetry            1
 Potential[kcal/mol]           18
   0.00    0.33    1.12    1.21    0.41    0.01    0.25    1.01    1.44    1.25    0.88    0.72    0.72    0.85    1.20
   1.44    1.12    0.33
 End


    Frequencies[1/cm]           26
   3264.4      3181.9      3166.9      3153.9      2981.5      2849.3      1527.9      1505.1      1387.0      1352.1
   1290.0      1249.5      1200.5      1145.4      1094.9      1056.4      996.69      954.87      838.72      813.40
   730.42      551.83      497.88      433.33      258.08      168.83
  ZeroEnergy[kcal/mol]             0.
  ElectronicLevels[1/cm]                    1
   0.0000000000000000        3.0000000000000000
 End
 End
 !************************************
Well W2
 Species
 RRHO
 Geometry[angstrom]            11
  C       0.000000000000     0.000000000000     0.000000000000
  C       0.000000000000     0.000000000000     1.486400000000
  C       1.439463090629     0.000000000000     2.013399450396
  H      -0.148236362138    -0.922408549564    -0.540641108899
```

```
 H        0.228777675422     0.912021396144    -0.531907734673
 C        1.887307090677    -0.890971421977     2.882083470532
 H       -0.503593123621    -0.892596974303     1.880719942822
 H        2.068697725902     0.786903481845     1.618152724879
 H        2.919202557695    -0.882007580107     3.206407821587
 H        1.244384802223    -1.660878364341     3.289146710225
 O       -0.514504973360     1.157145802708     2.012220942587
          Core     RigidRotor
                   SymmetryFactor    1.00000000000000
          End
 Rotor                      Hindered
 Group    6   8   9  10
 Axis           3          2
 Symmetry           1
 Potential[kcal/mol]          18
   0.00    0.42    1.83    3.35    0.59    0.22    0.48    1.36    1.77    2.50    1.92    1.74    1.88    2.32    2.71
   2.54    1.43    0.42
 End
    Frequencies[1/cm]          26
  3293.9      3252.7      3202.8      3173.0      3161.9      2997.1      1694.6      1443.2      1426.2      1348.6
  1318.7      1268.6      1165.0      1086.8      1031.6      1022.2      984.02      902.50      848.64      663.71
  525.89      512.13      360.25      349.16      282.12      168.12
 ZeroEnergy[kcal/mol]            0.
 ElectronicLevels[1/cm]                  1
 0.000000000000000E+000   3.00000000000000
 End
 End
 !************************************
Well W3
 Species
 RRHO     ! transition state
 Geometry[angstrom]            11
 C    0.00087   0.00395   0.00350
 C    0.00287  -0.00476   1.47851
 C    1.24174  -0.00469   2.24894
 C    1.37089  -0.63874   3.54363
 H   -0.86566  -0.43402   1.96713
 H    2.08294   0.52857   1.81353
 H    1.18632  -0.09065   4.46147
 H    1.69110  -1.67009   3.64379
 O   -0.29292   1.18079   0.71872
 H    0.95091   0.00165  -0.52176
 H   -0.83287  -0.44605  -0.52658
          Core     RigidRotor
                   SymmetryFactor    1.0000000000000000
          End
    Frequencies[1/cm]          27
  64.625      266.45      295.78      421.77      470.83      508.88      633.74      801.32      857.46      940.83
  959.00      1078.2      1108.2      1163.3      1175.6      1201.3      1275.2      1288.3      1443.1      1451.2
  1526.2      3096.4      3113.9      3133.6      3147.5      3187.8      3200.5
 ZeroEnergy[kcal/mol]           $wellpen
 ElectronicLevels[1/cm]                  1
  0.0000000000000000       3.0000000000000000
 End
 End
 !************************************
```

```
Barrier TS1
 RRHO    ! transition state
 Geometry[angstrom]            11
 C    0.00000   0.00000   0.00000
 C    0.00000   0.00000   1.34473
 C    1.20279   0.00000   2.14988
 H   -0.92019   0.04690  -0.56352
 H    0.92305   0.04916  -0.56210
 C    1.19663  -0.01751   3.48136
 H   -0.94562  -0.02081   1.87512
 H    2.14736   0.01299   1.61615
 H    2.11490  -0.01657   4.05129
 H    0.26799  -0.03478   4.03850
 O   -0.10163  -2.29724  -0.04848
          Core     RigidRotor
                   SymmetryFactor    0.5000000000000000
          End
 Rotor                      Hindered
 Group    6   8   9  10
 Axis           3          2
 Symmetry           1
 Potential[kcal/mol]          18
   0.00    0.66    2.41    4.83    5.92    5.17    3.63    2.45    2.42    3.14    2.69    2.59    3.55    5.12    6.03
4.96    2.60
 0.69
 End

    Frequencies[1/cm]          25
  3254.9      3250.8      3176.3      3168.3      3164.9      3155.7      1693.9      1634.3      1481.4      1416.2
  1330.5      1316.4      1237.0      1050.8      1009.2      997.80      968.86      964.85      908.44      781.35
  565.07      524.02      300.20      182.24      102.27
 ZeroEnergy[kcal/mol]              -0.54
 ElectronicLevels[1/cm]                  1
  0.0000000000000000       3.0000000000000000
 End
 End
 !************************************
Barrier TS2
 RRHO    ! transition state
 Geometry[angstrom]            11
 C        0.000000000000      0.000000000000      0.000000000000
 C        0.000000000000      0.000000000000      1.446351424719
 C        1.178314641204      0.000000000000      2.189202354961
 O       -1.032513430906      0.184193647439     -0.666209136615
 H        0.988668637599      0.088299051901     -0.484526528081
 C        1.225947762809      0.004032989263      3.552079818855
 H       -0.965759260329     -0.003982783482      1.936659509488
 H        2.115227759731     -0.004276002005      1.639880413971
 H        2.166813789808      0.003325533630      4.082359760907
 H        0.318187029448      0.008885168454      4.141021258855
 H        0.129124433760     -1.693080480756     -0.463145834508
          Core     RigidRotor
                   SymmetryFactor    1.00000000000000
          End
    Frequencies[1/cm]          26
  138.15      208.46      223.90      466.72      497.50      538.33      549.02      587.26      818.78      894.47
```

```
  976.46      1012.4      1037.6      1152.4      1221.5      1293.1      1298.3      1394.0      1489.4      1523.6
  1578.4      2939.4      3155.1      3163.7      3193.5      3262.7
 ZeroEnergy[kcal/mol]              16.76
 ElectronicLevels[1/cm]                  1
 0.000000000000000E+000   3.00000000000000
     Tunneling    Eckart
   ImaginaryFrequency[1/cm]      1020.10440000000
   WellDepth[kcal/mol]          16.76
   WellDepth[kcal/mol]          16.76
End
End
!************************************
Barrier TS3 REACS PRODS
 RRHO     ! transition state
 Geometry[angstrom]             11
 C    0.00000   0.00000   0.00000
 C    0.00000   0.00000   2.22666
 C    1.19578   0.00000   2.88222
 C    2.44330   0.15360   2.32501
 H   -1.02470  -0.10086   2.54631
 H    1.13301  -0.13919   3.96227
 H    3.32447   0.12783   2.94815
 H    2.56157   0.31652   1.26340
 O    0.79705   0.85242  -0.34984
 H    0.29006  -1.06169   0.07651
 H   -1.08278   0.20630   0.02610
       Core    RigidRotor
            SymmetryFactor    1.0000000000000000
       End
 Rotor                        Hindered
 Group   9 10 11
 Axis            1          2
 Symmetry           1
 Potential[kcal/mol]          18
   0.00    0.02    0.05    0.04    0.01    0.02    0.29    0.91    1.33    1.21    0.84    0.56    0.62    0.96    1.30
1.26    0.71
 0.16
 End
    Frequencies[1/cm]          25
  3275.5      3251.9      3170.4      3091.7      2982.0      2922.1      1682.7      1515.7      1501.2      1419.6
  1260.7      1254.0      1207.5      1100.1      1030.4      923.14      909.53      854.74      593.87      546.34
  522.16      486.97      273.68      144.50      142.12
 ZeroEnergy[kcal/mol]              22.51
 ElectronicLevels[1/cm]                  1
  0.0000000000000000        3.0000000000000000
     Tunneling    Eckart
   ImaginaryFrequency[1/cm]      260.10000000000002
   WellDepth[kcal/mol]          22.51
   WellDepth[kcal/mol]          12.55
End
End
!************************************
 Barrier TS4 REACS WP
 RRHO     ! transition state
 Geometry[angstrom]             11
 C         0.000000000000       0.000000000000       0.000000000000
```

```
C       0.000000000000      0.000000000000      1.360204187449
C       1.236420960526      0.000000000000      2.141928742491
H      -0.918629166807     -0.092086310583     -0.560308859280
H       0.915216889322      0.159549790611     -0.553855057696
C       1.265815067664     -0.166493698316      3.458645523374
H      -0.910019443540     -0.244076856904      1.892054117170
H       2.156462195292      0.157441471397      1.590371361826
H       2.196872939222     -0.160218431085      4.007492375581
H       0.355383347700     -0.310544125567      4.027004699785
O      -0.233542653576      2.000967293530      1.558263997808
      Core    RigidRotor
           SymmetryFactor   0.50000000000000000
      End
Rotor                      Hindered
Group    6   8   9  10
Axis           3          2
Symmetry           1
Potential[kcal/mol]          18
   0.00    0.42    1.94    3.96    4.85    3.97    2.38    1.48    1.64    1.92    1.69    1.96    3.24    4.50    4.93
4.16    2.32
 0.63
End
    Frequencies[1/cm]          25
  3268.0      3256.4      3206.5      3182.8      3168.3      3163.5      1723.1      1577.8      1477.3      1405.5
  1331.9      1295.7      1231.5      1030.7      1009.9      994.66      963.81      900.58      885.93      700.20
  521.78      514.09      307.23      232.92      77.250
 ZeroEnergy[kcal/mol]               0.35
 ElectronicLevels[1/cm]                   1
  0.0000000000000000        3.0000000000000000
     Tunneling    Eckart
   ImaginaryFrequency[1/cm]      381.56000000000000
   WellDepth[kcal/mol]          0.35
   WellDepth[kcal/mol]          18.87
End
End
!************************************
 Barrier TS5 REACS WR
RRHO     ! transition state
Geometry[angstrom]             11
C    0.00000   0.00000   0.00000
C    0.00000   0.00000   1.31630
C    1.06551   0.00000   2.29340
H   -0.91871   0.00000  -0.56987
H    0.93522  -0.00000  -0.55264
C    0.88633   0.00000   3.60895
H   -1.19233   0.00000   1.85067
H    2.07075  -0.00000   1.87821
H    1.72932   0.00000   4.28486
H   -0.10688   0.00000   4.03871
O   -2.29026   0.00000   2.31196
          Core     RigidRotor
                   SymmetryFactor    1.0000000000000000
          End
Rotor                      Hindered
Group    6   8   9  10
Axis           3          2
```

```
 Symmetry           1
 Potential[kcal/mol]          18
   0.00    0.42    1.48    2.45    2.55    1.93    1.34    1.42    2.33    3.04    2.33    1.42    1.34    1.93    2.55
2.45    1.48
 0.42
 End
    Frequencies[1/cm]          25
  3260.3      3234.2      3166.9      3135.2      3128.9      1739.9      1682.5      1460.0      1415.4      1318.2
  1224.5      1082.2      1016.0      995.12      988.17      959.18      923.38      892.99      739.82      576.90
  492.79      457.77      264.69      248.24      112.30
 ZeroEnergy[kcal/mol]               7.65
 ElectronicLevels[1/cm]                   1
  0.0000000000000000        6.0000000000000000
     Tunneling    Eckart
   ImaginaryFrequency[1/cm]      1532.1400000000001
   WellDepth[kcal/mol]          7.65
   WellDepth[kcal/mol]          7.65
End
End
!************************************
 Barrier TS6 REACS WP
RRHO     ! transition state
Geometry[angstrom]             11
 C         0.000000000000      0.000000000000      0.000000000000
 C         0.000000000000      0.000000000000      1.434152619110
 O         1.087469193795      0.000000000000      2.071213305400
 H         0.917501611357      0.223888152947     -0.524781782173
 H        -0.898353879127     -0.226477148671     -0.556263894219
 H        -0.909247645356     -0.379007235461      1.923495232740
 C        -0.616871765084      1.938025491914      2.032706402918
 C        -0.789170778170      2.817125648040      1.086742029839
 H        -0.707716003131      1.946283504620      3.106509461612
 H        -0.596264436222      2.577248153574      0.045573134606
 H        -1.134252312516      3.823769448344      1.305886626521
          Core     RigidRotor
                   SymmetryFactor    1.00000000000000
          End
 Rotor                        Hindered
 Group    8   9  10  11
 Axis             7          2
 Symmetry           1
 Potential[kcal/mol]          18
   0.00    0.17    0.63    1.00    0.97    0.78    0.74    0.89    1.07    1.14    1.04    0.95    0.92    0.89    0.85
0.78    0.53
 0.18
 End
    Frequencies[1/cm]          25
  3280.4      3269.2      3191.1      3163.8      3114.1      2981.9      1675.3      1483.5      1460.5      1394.3
  1347.3      1155.1      1109.2      964.14      943.56      920.99      882.54      823.05      710.93      515.43
  425.70      393.03      338.52      238.05      172.33
 ZeroEnergy[kcal/mol]               6.59
 ElectronicLevels[1/cm]                   1
 0.000000000000000E+000   3.00000000000000
     Tunneling    Eckart
   ImaginaryFrequency[1/cm]      391.140000000000
   WellDepth[kcal/mol]          6.59
```

```
   WellDepth[kcal/mol]          14.50
 End
 End
!************************************
Barrier TS7 REACS WP
 RRHO     ! transition state
 Geometry[angstrom]             11
 C        0.000000000000      0.000000000000      0.000000000000
 C        0.000000000000      0.000000000000      1.478821264963
 C        1.159222139269      0.000000000000      2.222354789373
 C        1.202455532189      0.068884285640      3.674711570643
 H       -0.962389152117      0.012891969772      1.967963617072
 H        2.100769660868     -0.001673289559      1.675749645188
 H        1.314953390385      1.021583993360      4.176735197866
 H        1.219853622156     -0.828095936499      4.279698965100
 O       -0.042353437516      1.342424930646      0.295305547044
 H        0.915081410725     -0.352765852500     -0.483260332456
 H       -0.897892695678     -0.409501271595     -0.467654917747
          Core     RigidRotor
                   SymmetryFactor    1.00000000000000
          End
    Frequencies[1/cm]          26
  166.98      254.57      275.57      373.38      438.39      523.50      720.39      901.99      984.11      989.07
  1035.2      1110.1      1168.1      1212.8      1273.8      1291.0      1300.8      1441.1      1495.6      1532.5
  3026.9      3089.1      3115.8      3140.4      3226.8      3237.7
 ZeroEnergy[kcal/mol]             0.
 ElectronicLevels[1/cm]                   1
 0.000000000000000E+000   3.00000000000000
     Tunneling    Eckart
   ImaginaryFrequency[1/cm]      513.079300000000
   WellDepth[kcal/mol]        0.
   WellDepth[kcal/mol]        0.
 End
 End
 !************************************
Barrier TS8 REACS WP
 RRHO     ! transition state
 Geometry[angstrom]             11
 C    0.00000   0.00000   0.00000
 C    0.00000   0.00000   1.47166
 C    1.28664   0.00000   2.24031
 H   -0.57044  -0.73227  -0.55085
 H    0.51559   0.78095  -0.53920
 C    2.48344   0.42240   1.73119
 H   -0.72033  -0.70941   1.88891
 H    1.22071  -0.36395   3.25470
 H    3.37117   0.42930   2.34637
 H    2.56583   0.78330   0.71654
 O   -0.00608   1.23826   2.09099
          Core     RigidRotor
                   SymmetryFactor    1.0000000000000000
          End
 Rotor                      Hindered
 Group    8   9  10  11
 Axis           7          2
 Symmetry           1
```

```
 Potential[kcal/mol]          18
   0.00    0.17    0.63    1.00    0.97    0.78    0.74    0.89    1.07    1.14    1.04    0.95    0.92    0.89    0.85
0.78    0.53
 0.18
 End
    Frequencies[1/cm]          26
  130.79      235.19      295.70      401.18      513.98      531.13      590.10      841.40      848.10      925.25
  972.89      1048.9      1112.2      1164.7      1237.2      1294.0      1403.5      1407.3      1476.0      1531.1
  3042.7      3169.7      3173.6      3223.9      3272.4      3282.6
 ZeroEnergy[kcal/mol]              4.87
 ElectronicLevels[1/cm]                   1
  0.0000000000000000        3.0000000000000000
     Tunneling    Eckart
   ImaginaryFrequency[1/cm]      501.97910000000002
   WellDepth[kcal/mol]          4.87
   WellDepth[kcal/mol]          2.24
 End
 End
 !************************************
Barrier TS10 REACS PRODS
 RRHO     ! transition state
 Geometry[angstrom]             11
 C    0.00000   0.00000   0.00000
 C    0.00000   0.00000   1.43664
 C    1.28636   0.00000   2.20568
 H    0.90096  -0.10268  -0.58480
 H   -0.94961   0.10197  -0.50228
 C    2.50750  -0.06274   1.69571
 H   -0.20094  -1.62798   1.89476
 H    1.13628   0.08327   3.27514
 H    3.37562  -0.03393   2.33927
 H    2.69593  -0.14456   0.63366
 O   -1.05923   0.33457   2.03517
          Core     RigidRotor
                   SymmetryFactor    1.0000000000000000
          End
 Rotor                      Hindered
 Group    8   9  10  11
 Axis           7          2
 Symmetry           1
 Potential[kcal/mol]          18
   0.00    0.17    0.63    1.00    0.97    0.78    0.74    0.89    1.07    1.14    1.04    0.95    0.92    0.89    0.85
0.78    0.53  0.18
 End
    Frequencies[1/cm]          26
  79.918      303.99      325.76      392.06      480.97      501.68      515.94      619.81      690.61      779.25
  836.42      982.44      994.08      1045.7      1068.3      1305.4      1318.9      1427.0      1470.0      1486.2
  1721.1      3166.1      3180.4      3193.3      3251.6      3293.6
 ZeroEnergy[kcal/mol]             13.22
 ElectronicLevels[1/cm]                   1
  0.0000000000000000        3.0000000000000000
     Tunneling    Eckart
   ImaginaryFrequency[1/cm]      1051.0806000000000
   WellDepth[kcal/mol]          0.01
   WellDepth[kcal/mol]          0.01
 End
```

```
 End
 !************************************
!************************************
Barrier MECP REACS PRODS
 RRHO    ! transition state
 Geometry[angstrom]            11
  C                  0.000000    0.000000    0.000000
  C                  0.000000    0.000000    1.496202
  C                  1.158853    0.000000    2.246685
  O                 -0.510920   -1.193219   -0.450116
  H                 -0.679179    0.783987   -0.378834
  H                  0.999067    0.205698   -0.406429
  O                  1.197611   -0.030153    3.620032
  H                 -0.964375   -0.074963    1.984070
  H                 2.102252    0.038882    1.710024
  H                 2.135194   -0.010547    4.155274
  H                 0.286678   -0.073502    4.202259
          Core     RigidRotor
                   SymmetryFactor    1.0000000000000000
          End
Rotor                      Hindered
 Group  4 5 6
 Axis           1          2
 Symmetry           1
 Potential[kcal/mol]          18
   0.00    0.33    1.12    1.21    0.41    0.01    0.25    1.01    1.44    1.25    0.88    0.72    0.72    0.85    1.20
1.44    1.12
 0.33
 End
    Frequencies[1/cm]          25
  3262.6      3184.0      3162.8      3148.8      3004.1      2867.0      1523.8      1498.9      1422.2      1357.3
  1294.0      1216.3      1197.3      1113.2      1074.3      1010.1      986.79      954.88      837.20      760.35
  633.63      554.31      483.81      285.10      177.59
 ZeroEnergy[kcal/mol]              0.
 ElectronicLevels[1/cm]                   1
  0.0000000000000000        3.0000000000000000
End
 !************************************
```

REFERENCES

1 M. Alagia, V. Aquilanti, D. Ascenzi, N. Balucani, D. Cappelletti, L. Cartechini, P. Casavecchia, F. Pirani, G. Sanchini and G. G. Volpi, *Isr. J. Chem.*, 1997, **37**, 329-342.

2 F. Leonori, N. Balucani, G. Capozza, E. Segoloni, G. G. Volpi and P. Casavecchia, *Phys. Chem. Chem. Phys.,* 2014, **16**, 10008 – 10022.

3 P. Casavecchia, *Rep. Prog. Phys.*, 2000, **63**, 355-414.

4 P. Casavecchia, F. Leonori and N. Balucani, *Int. Rev. Phys. Chem.*, 2015, **34**, 161-204.

5 R. D. Levine, *Molecular Reaction Dynamics*, Cambridge University Press, 2005.

6 W. B. Miller, S. A. Safron and D. R. Herschbach, *Discuss. Faraday Soc.*, 1967, **44**, 108-123.

7 G. A. Fisk, J. D. McDonald and D. R. Herschbach, General discussion*, Discuss. Faraday Soc.*, 1967, **44**, 228-230.

8 A. Caracciolo, P. Recio, N. Balucani, M. Rosi, C. Cavallotti and P. Casavecchia, work in progress.

9 P. Casavecchia, K. Liu and X. Yang, Reactive scattering: reactions in three dimensions. In: *Tutorials in Molecular Reaction Dynamics*, Mark Brouard & Claire Vallance, eds. (Royal Society of Chemistry Publishing, Cambridge, UK), Ch. VI (2010), pp. 167-213.